12-10-2005

X-Ray Imaging of Planetary Nebulae with Wolf-Rayet-type Central Stars: Detection of the Hot Bubble in NGC 40

Rodolfo Montez Jr.
University of Rochester

Joel H. Kastner
Rochester Institute of Technology

Orsola De Marco
American Museum of Natural History

Noam Soker
Technion-Israel Institute of Technology

Recommended Citation
Rodolfo Montez, Jr. et al 2005 ApJ 635 381 https://doi.org/10.1086/497262

The Astrophysical Journal, 635:381–385, 2005 December 10

X-RAY IMAGING OF PLANETARY NEBULAE WITH WOLF-RAYET–TYPE CENTRAL STARS: DETECTION OF THE HOT BUBBLE IN NGC 40

Rodolfo Montez, Jr.,[1] Joel H. Kastner,[2] Orsola De Marco,[3] and Noam Soker[4]

Received 2005 June 24; accepted 2005 August 15

ABSTRACT

We present the results of *Chandra X-Ray Observatory* observations of the planetary nebulae (PNs) NGC 40 and Hen 2-99. Both PNs feature late-type Wolf-Rayet central stars that are currently driving fast ($\sim$1000 km s^{-1}), massive winds into denser, slow-moving ($\sim$10 km s^{-1}) material ejected during recently terminated asymptotic giant branch (AGB) evolutionary phases. Hence, these observations provide key tests of models of wind-wind interactions in PNs. In NGC 40, we detect faint, diffuse X-ray emission distributed within a partial annulus that lies nested within a $\sim$40″ diameter ring of nebulosity observed in optical and near-infrared images. Hen 2-99 is not detected. The inferred X-ray temperature ($T_X \sim 10^6$ K) and luminosity ($L_X \sim 2\times10^{30}$ ergs s^{-1}) of NGC 40 are the lowest measured thus far for any PN displaying diffuse X-ray emission. These results, combined with the ringlike morphology of the X-ray emission from NGC 40, suggest that its X-ray emission arises from a ''hot bubble'' that is highly evolved and is generated by a shocked, quasi-spherical fast wind from the central star, as opposed to AGB or post-AGB jet activity. In contrast, the lack of detectable X-ray emission from Hen 2-99 suggests that this PN has yet to enter a phase of strong wind-wind shocks.

Subject headings: planetary nebulae: general — planetary nebulae: individual (NGC 40, Hen 2-99) — stars: winds, outflows — stars: Wolf-Rayet — X-rays: ISM

Online material: color figure

1. INTRODUCTION

Planetary nebulae (PNs) are the descendents of intermediate (1–8 $M_\odot$) mass stars. The central star of a PN will evolve into a white dwarf with a mass between $\sim$0.55 and $\sim$1.0 $M_\odot$. While on the upper asymptotic giant branch (AGB), much of the star's initial mass is lost in a more or less spherical outflow at rates of up to $10^{-4}\,M_\odot$ yr^{-1} and at speeds of $\sim$10–20 km s^{-1}. As the star leaves the AGB, the UV radiation from the emerging white dwarf (WD) ionizes the red giant ejecta, producing the short-lived ($\sim3\times10^4$ yr) PN. The star's surface escape velocity also increases at this stage, and its wind speed may increase to $\sim$1000 km s^{-1} as its mass-loss rate drops to $\sim10^{-8}\,M_\odot$ yr^{-1}. This fast wind is shocked as it collides with the previously ejected slow wind. This process is expected to play a role in PN shaping.

These same wind-wind shocks are energetic enough to generate X-ray emission and, with the advent of the *Chandra X-Ray Observatory* and *XMM-Newton*, diffuse X-ray emission indeed has been detected in several PNs (Kastner et al. 2000, 2001, 2002, 2003; Chu et al. 2001; Guerrero et al. 2002, 2005). However, the degree to which wind-wind interactions contribute to PN X-ray emission likely varies from object to object. In particular, some PNs display X-ray ''hot bubbles,'' as predicted by wind-wind interaction models (e.g., BD +30 3639, Kastner et al. [2003]; NGC 7009, Guerrero et al. [2002]), whereas the X-ray morphologies of other PNs indicate that their X-ray emission is a direct consequence of jet activity (e.g., He 3-1475, Sahai et al. [2003]; Hen 2-154 [Mz 3], Kastner et al. [2003]).

Planetary nebulae harboring relatively cool, WC-type Wolf-Rayet central stars (typically designated [WCL] objects, where L differentiates the cooler, later objects from the earlier [WCE] objects; e.g., Leuenhagen et al. 1996) represent important test cases for understanding the origin and nature of X-ray emission from PNs. The WC central stars of PNs are characterized by their overall spectral resemblance to ''bona fide,'' massive WR stars, but as a group they extend to both hotter and cooler effective temperatures (Gorny & Tylenda 2000). The luminosities determined for the WC central stars of PNs, given reasonable distance estimates, confirm that these stars are much less luminous than the WC remnants of massive stars and establish beyond doubt their post-AGB nature.

Key properties of the [WCL]s indicate they should offer prime examples of strong wind-wind interactions in PNs. The [WC] central stars exhibit extreme hydrogen deficiency, similar to that of their likely progeny, the PG 1159–type pulsating white dwarfs (Koesterke et al. 1998). By virtue of the high opacity characteristic of a C- and O-enriched, yet H-depleted gas mix (De Marco & Barlow 2001), the [WCL] central stars develop powerful winds characterized by mass-loss rates $\sim10^{-6}\,M_\odot$ yr^{-1} (Leuenhagen et al. 1996). The central star wind velocities of [WCL]s range from $\sim$200 to $\sim$1000 km s^{-1} and appear to correlate with spectral type, the coolest [WCL]s having the lowest wind speeds (Leuenhagen et al. 1996). These velocities are unusually large for such relatively cool central stars. The very large stellar wind momenta of PNs with WC central stars appear to result in systematically larger nebular expansion velocities among these objects, relative to PNs with H-rich central stars (Gorny & Stasinska 1995). Furthermore, as a group, the [WCL] PNs are characterized by dense, blobby structures and are rich in dust and molecular gas. These nebulae also tend to be relatively compact; most feature optically bright shells with radii $<$3000 AU (Gorny & Tylenda 2000) which, given typical late-AGB expansion velocities ($\sim$15–30 km s^{-1}), suggest that they are quite young (dynamical ages $<$1000 yr).

[1] Department of Physics and Astronomy, University of Rochester, Rochester, NY 14627; rudy@pas.rochester.edu.

[2] Chester F. Carlson Center for Imaging Science, Rochester Institute of Technology, 54 Lomb Memorial Drive, Rochester, NY 14623; jhk@cis.rit.edu.

[3] Department of Astrophysics, American Museum of Natural History, Central Park West at 79th Street, New York, NY 10024; orsola@amnh.org.

[4] Department of Physics, Technion-Israel Institute of Technology, 32000 Haifa, Israel; soker@physics.technion.ac.il.

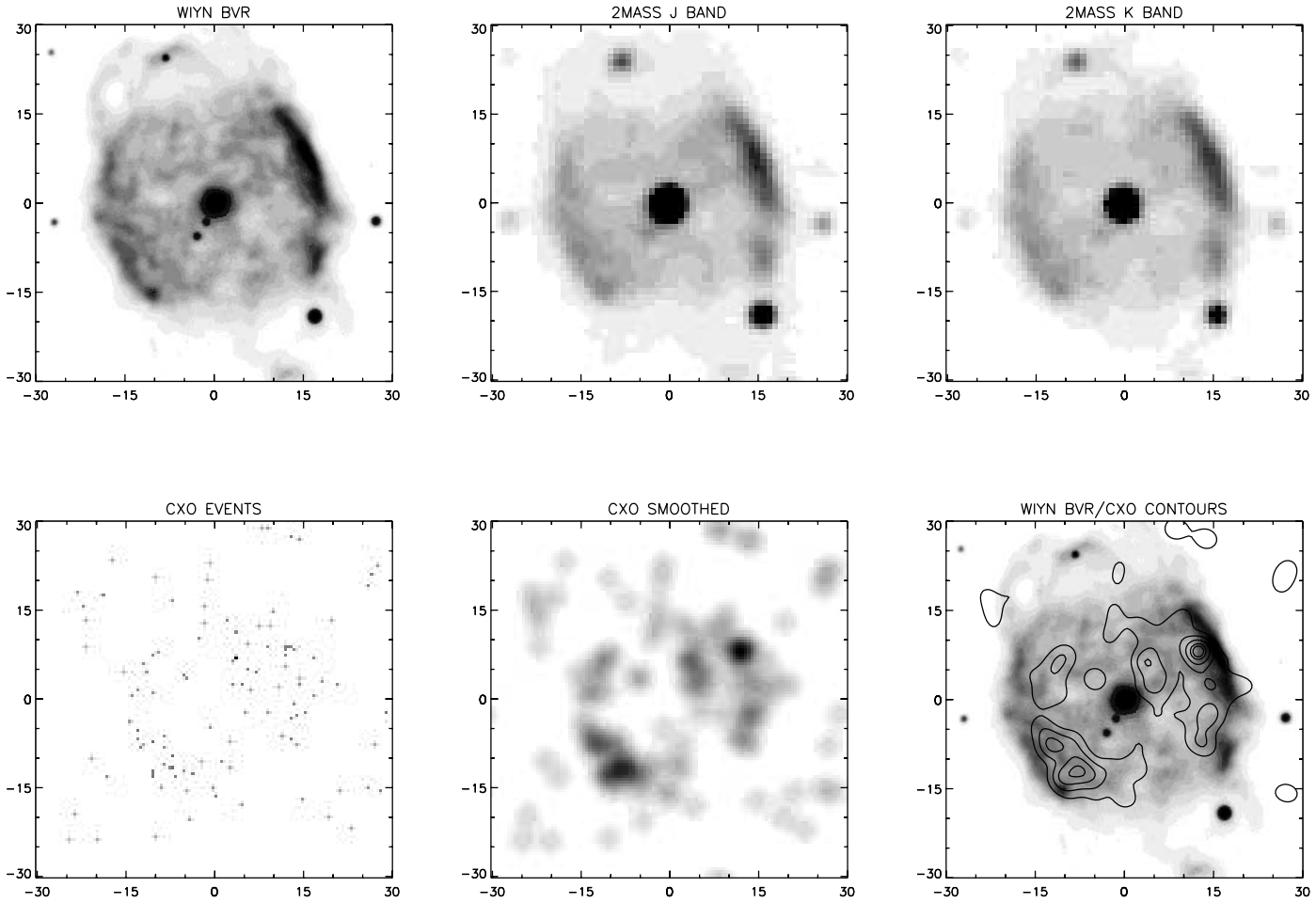

FIG. 1.—Optical, near-infrared, and X-ray images of NGC 40. *Top row, left to right:* WIYN *BVR* composite image (converted to gray scale) and 2MASS *J*- and *K*-band images. *Bottom row, left to right: Chandra* X-ray and smoothed (see below) *Chandra* X-ray images, and contours of the smoothed *Chandra* X-ray image overlaid on the WIYN *BVR* composite gray-scale image. The images are $60'' \times 60''$ with north up and east to the left. The 2MASS images are displayed on a linear gray scale. The smoothed *Chandra* X-ray images in this figure and in Fig. 5 were obtained by convolving the original image with a PSF with FWHM $\sim 4''$. The contours of the *Chandra* X-ray image in the lower right panel are at 20%, 40%, 60%, 80%, and 90% of the image maximum of 1.6×10^{-3} counts ks^{-1} arcsec^{-2} (0.3–1.0 keV).

Taken together, the foregoing suggests that the H abundances of [WCL]s sharply declined just at the end of their AGB evolution (Herwig 2001). Hence, these stars have acquired large envelope opacities, resulting in strong winds—much stronger than in normal, H-rich central stars of PNs. Furthermore, the strong winds have emerged very early in post-AGB evolution, before the remnant, ejected AGB envelope has had time to disperse into the interstellar medium. Thus, the [WCL] PNs should make ideal tests for the theory of production of X-rays via interacting wind shocks, as the very large wind momenta of [WCL] central stars and the large, lingering masses of AGB ejecta in [WCL] PNs should offer precisely the right conditions for production of hot, postshock gas at high emission measure. Furthermore, the blobby and/or filamentary structure of [WCL] PNs should favor heat conduction and mixing of "hot bubble" and nebular gas (Soker & Kastner 2003).

Indeed, among the prototype [WCL] objects is BD +30 3639, the first well-established—and brightest—example of diffuse X-ray emission from a PN (Kreysing et al. 1992; Arnaud et al. 1996; Kastner et al. 2000, 2002; Soker & Kastner 2003). The central star within the second-brightest diffuse X-ray PN, NGC 6543, also has long been classified as Wolf-Rayet type (Swings 1940). Its wind speed and mass-loss rate (1750 km s^{-1} and $\sim 10^{-7}\ M_\odot$ yr^{-1}, respectively; Perinotto et al. 1989) are quite large, explaining the star's broad emission line spectrum. However, most of the key optical emission lines characteristic of the WC central stars of PNs (Crowther et al. 1998) are not present in the spectrum of the central star of NGC 6543 and the star is not H deficient (Mendez et al. 1988). Therefore, a [WC] classification is precluded. Nevertheless, NGC 6543 may represent a transient stage in the evolution of [WC] PNs, as its central star may belong to a potentially related, "weak emission line" class (Acker et al. 1996; Pena et al. 2001).

Additional X-ray observations of [WC] PNs should further clarify the role of post-AGB fast winds in generating diffuse X-ray emission within PNs. To this end, we used *Chandra* to search for X-ray emission from two well-studied [WC] PNs, NGC 40 (central star spectral type [WC8], fast wind speed $v_f = 1000$ km s^{-1}; Leuenhagen et al. 1996) and Hen 2-99 ([WC9], $v_f = 900$ km s^{-1}). The low-resolution optical morphologies (e.g., Kaler et al. 1989), central star spectral types, fast wind speeds, and (large) central star mass-loss rates ($\sim 3 \times 10^{-6}\ M_\odot$ yr^{-1}; Leuenhagen et al. 1996) of these two PNs bear close resemblance to BD +30 3639 ([WC9], $v_f = 700$ km s^{-1}, Leuenhagen et al. [1996]; mass-loss rate $\sim 10^{-6}\ M_\odot$ yr^{-1}, Soker & Kastner [2003]). Unlike BD +30 3639 and NGC 6543, both of which have been the subject of intensive, multiepoch observing campaigns by the *Hubble Space Telescope* (*HST*; Balick & Hajian

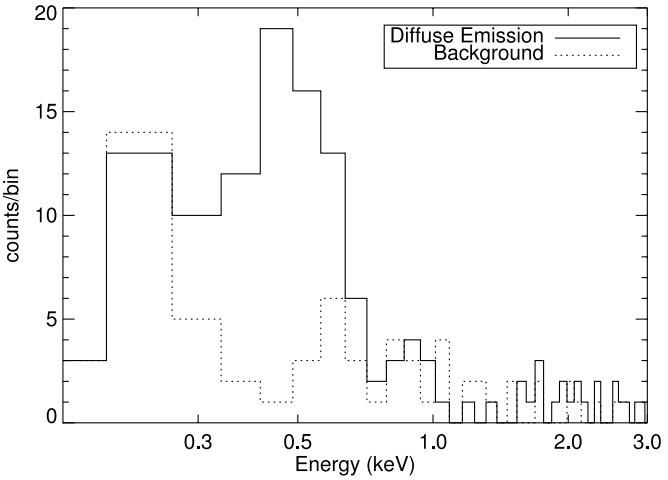

FIG. 2.—"Raw" (counts vs. energy) X-ray spectrum of NGC 40 (*solid histogram*), extracted from the region encompassed by the optical/near-IR nebula (the raw background spectrum is displayed as a dotted histogram).

2004; Li et al. 2002), neither NGC 40 nor Hen 2-99 has been the subject of deep *HST* imaging.

2. OBSERVATIONS AND RESULTS

Chandra observed Hen 2-99 and NGC 40 with the back-illuminated CCD S3 of the Advanced CCD Imaging Spectrometer (ACIS) as the focal plane instrument, on 2003 November 12 (ObsID 4480) and 2004 June 13 (ObsID 4481), respectively. Exposure times were 29 ks for Hen 2-99 and 20 ks for NGC 40. ACIS has a pixel size of 0.″49 and the field of view of ACIS-S3 is $\sim 8' \times 8'$. The *Chandra*/ACIS combination is sensitive over the energy range 0.3–10 keV. The data were subject to standard processing by the Chandra X-Ray Center pipeline software (CIAO, ver. 2.3). We further applied energy-dependent subpixel event position corrections appropriate for back-illuminated CCD ACIS-S3 (Li et al. 2003).

2.1. *NGC 40*

In Figure 1 we present WIYN[5] optical (composite *BVR*) and 2MASS[6] near-infrared (*J*- and *K*-band) images of NGC 40 along with the narrow-band (0.3–1 keV) *Chandra*/ACIS X-ray image (raw and smoothed) of the same region. The morphology of the $\sim$40″ diameter nebula is similar in these three optical/near-infrared images: in each case NGC 40 appears as a limb-brightened shell, with a bright rim that is interrupted by fainter protrusions to the north-northeast and south-southwest. Deep optical images reveal jetlike features in the vicinity of each protrusion, although there is no kinematical evidence for collimated, fast outflows in NGC 40 (Meaburn et al. 1996).

The detection of soft X-rays from NGC 40 is apparent upon extraction of a spectrum from a region of the *Chandra*/ACIS image encompassing the optical/near-infrared nebula. This spectrum is displayed in Figure 2. An image extracted over the soft (0.3–1.0 keV) energy range spanned by the detected photons reveals that the X-ray emission arises from an annular region that lies nested just within, and follows the overall surface brightness distribution of, the bright, partial rim seen in the optical and near-infrared (Figs. 1 and 3).

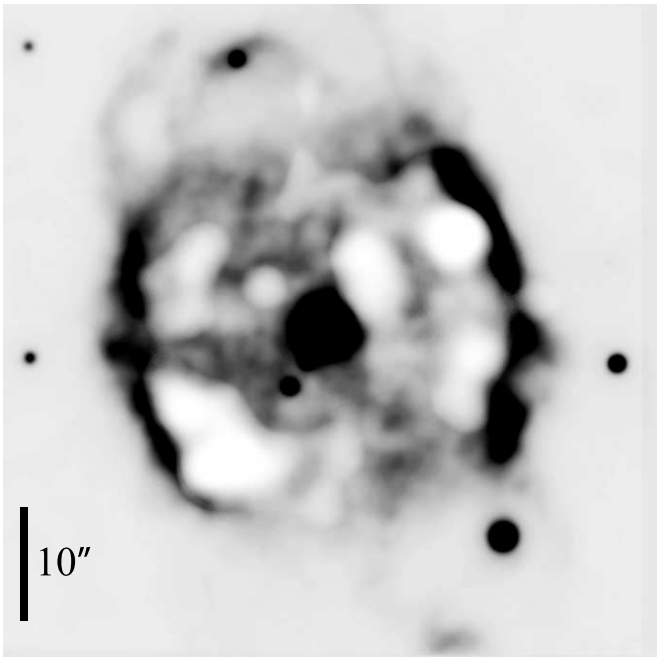

FIG. 3.—Overlay of WIYN BVR composite, 2MASS *K*-band (reverse greyscale), and CXO X-ray images (bright greyscale). [*See the electronic edition of the Journal for a color version of this figure.*]

Refining the spectral extraction region to an annulus with inner radius 4″ and outer radius of 20″ results in the background-subtracted spectrum displayed in Figure 4. The background-subtracted count rate of this diffuse emission was $(2.8 \pm 0.9) \times 10^{-3}$ counts s^{-1}, where the background region was defined as a circular region of radius $\sim$40″ lying $\sim$135″ southeast of NGC 40. We used XSPEC (ver. 12.2.0; Arnaud 1996) to fit the spectrum with a Raymond-Smith thermal plasma emission model suffering intervening absorption. Based on the inferred nebular color excess

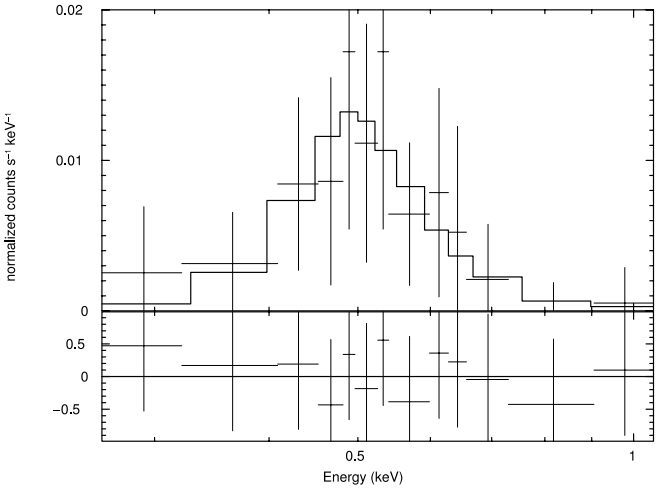

FIG. 4.—*Top plot*: Background-subtracted X-ray spectrum of NGC 40 (*crosses*), with best-fit thermal plasma model overlaid (*solid histogram*; see text). *Bottom plot*: Residuals of the fit in units of σ.

[5] The WIYN Observatory is owned and operated by the WIYN Consortium, which consists of the University of Wisconsin, Indiana University, Yale University, and the National Optical Astronomy Observatories (NOAO). NOAO is operated by the Association of Universities for Research in Astronomy (AURA), Inc. under cooperative agreement with the National Science Foundation. See http://www.noao.edu/wiyn/wiynimages.html.

[6] This publication makes use of data products from the Two Micron All Sky Survey, which is a joint project of the University of Massachusetts and the Infrared Processing and Analysis Center/California Institute of Technology, funded by the National Aeronautics and Space Administration and the National Science Foundation. (See http://www.ipac.caltech.edu/2mass/.)

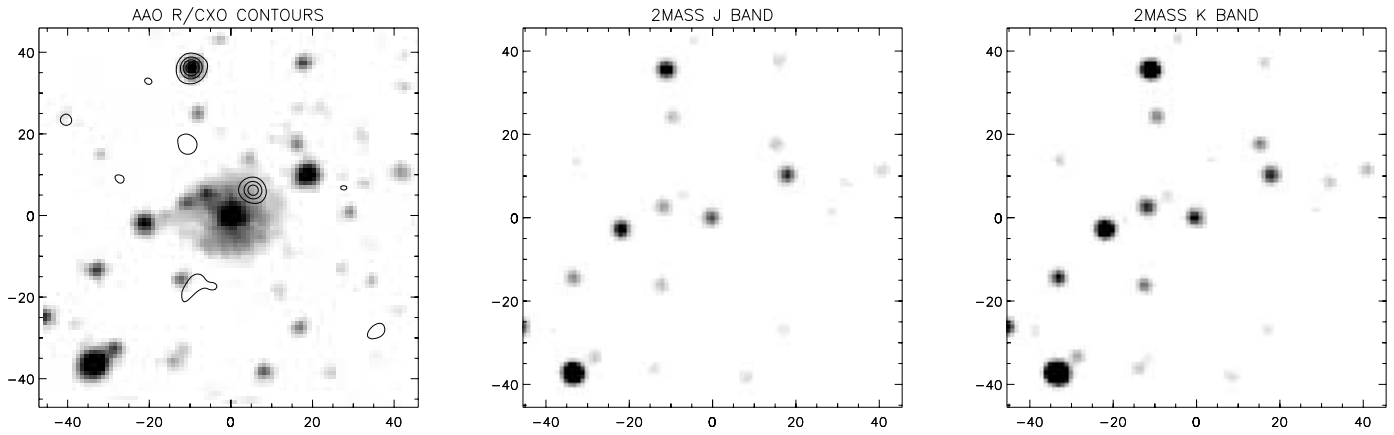

FIG. 5.—Optical, near-infrared, and X-ray images of the Hen 2-99 region. *Left:* AAO short *R*-band image, with smoothed *Chandra* X-ray image overlaid as a contour map. *Center:* 2MASS *J*-band image. *Right:* 2MASS *K*-band image. The images are $90'' \times 90''$ with north up and east to the left. The AAO and 2MASS images are presented as linear gray scale. The contours in the left panel are at 20%, 40%, 60%, 80%, and 90% of the X-ray image maximum of 0.14 counts ks^{-1} $arcsec^{-2}$ (0.3–10.0 keV).

of $E(B-V) = 0.38$ (Pottasch et al. 1977), we fixed the absorbing column at $N_H = 2.2 \times 10^{21}$ cm^{-2}. The best fit indicates a plasma temperature of $T_X \sim 8.0 \times 10^5$ K, with an uncertainty of $\sim$20%. The model fit is marginally improved by the inclusion of a Gaussian component at an energy 0.5 ± 0.2 keV, which is suggestive of the presence of excess O VII emission. The inclusion of this second component would imply a somewhat higher plasma temperature ($T_X \sim 1.5 \times 10^6$ K). The modeling indicates an unabsorbed X-ray flux $\sim 1.3 \times 10^{-14}$ ergs cm^{-2} s^{-1} (the mean of the flux from plasma components obtained by fits with and without the 0.5 keV Gaussian component), corresponding to an intrinsic X-ray luminosity $L_X \sim 1.5 \times 10^{30} (D/1.0 \text{ kpc})^2$ ergs s^{-1} where D is the distance to NGC 40. The estimate $D = 1.0$ kpc was determined by Leuenhagen et al. (1996).

2.2. *Hen 2-99*

In Figure 5 we present Anglo-Australian Observatory Digitized Sky Survey[7] Short *R*-band and 2MASS *J*- and *K*-band images of Hen 2-99 along with the broadband (0.3–10 keV) *Chandra*/ACIS X-ray image (raw and smoothed) of the same region. The object appears as a $\sim 25''$ diameter nebula in the *R*-band image, while only the central star is detected in the near-infrared image. Pointlike X-ray sources in the immediate vicinity of Hen 2-99, including one source that lies $\sim 6''$ from the central star and has no optical or near-infrared counterpart, have similar and relatively hard spectra, and are most likely background sources.

We searched for diffuse emission from Hen 2-99 via the same approach used for NGC 40, i.e., we extracted a 0.3–10 keV spectrum from the region of the *Chandra*/ACIS image encompassing the *R*-band emission from Hen 2-99. The spectral extraction avoided the point source that lies closest to the position of the central star. Upon subtraction of background emission within a region defined by a circle with radius $\sim 10''$, the resulting X-ray spectrum (not shown) reveals no source photons.

From the 1 σ uncertainty in the background count rate (2×10^{-3} counts s^{-1}) we find a (3 σ) upper limit on the unabsorbed X-ray luminosity of $L_X < 5 \times 10^{30} (D/2.5 \text{ kpc})^2$ ergs s^{-1}. The estimate $D = 2.5$ kpc was determined by Leuenhagen et al. (1996). For this upper limit, we (conservatively) assume an X-ray emission temperature at the upper end of the range determined thus far for the diffuse emission from PNs ($T_X = 3 \times 10^6$ K), and adopt $N_H = 2.9 \times 10^{21}$ cm^{-2} based on a color excess of $E(B-V) = 0.5$ (Leuenhagen et al. 1996).

3. DISCUSSION

The shell-like shape of the X-ray emitting region in NGC 40, and the correspondence of this region to the bright optical/near-IR rim in this nebula, indicates that the bright rim has been generated by the shocked fast wind from the central star. The lack of X-ray emission associated with the apparent "blowouts" (interruptions in the rim) that are aligned along an axis running NNE-SSW in NGC 40 further suggests that this wind is more or less spherically symmetric, with a possible enhancement along the equatorial plane of the system rather than along the polar axis. We note that there is no kinematic evidence for the presence of collimated jets in NGC 40, despite the appearance of polar "blowouts" and jetlike features in this nebula (Meaburn et al. 1996; Martin et al. 2002).

The X-ray morphology of NGC 40 appears similar to (but is better resolved than) those of BD +30 3639 (Kastner et al. 2000) and NGC 7009 (Guerrero et al. 2002). The appearances of these structures are fully consistent with the generation of "hot bubbles" via wind-wind interactions (Akashi et al. 2006). These X-ray morphologies stand in sharp contrast to the radially directed X-ray structures within the young planetary nebulae NGC 7027 and Mz 3, however. These two PNs display X-ray evidence for the action of collimated jets (Kastner et al. 2001, 2002, 2003; Cox et al. 2002), and in both cases the X-ray emission appears intimately associated with the ongoing structural changes apparent in the optical/near-infrared nebulae. Thus it appears that two quite different processes—jets on the one hand, and quasi-spherical fast winds on the other—may be responsible for energetic shocks, and hence high-temperature plasma in PNs (see also Guerrero et al. [2005] and Akashi et al. [2006]). It is clear, furthermore, that the different processes responsible for X-ray emission are closely tied to the different PN shapes that are seen in optical emission lines.

The inferred X-ray temperature and luminosity of NGC 40 ($T_X \sim 10^6$ K and $L_X \sim 1.5 \times 10^{30}$ ergs s^{-1}, respectively; § 2.1) are the lowest measured thus far for any PN (Soker & Kastner 2003; Kastner et al. 2003; Guerrero et al. 2005), and the radii of the bright rim and X-ray emitting shell in NGC 40 are $\sim$10 times larger than these same structures in BD +30 3639. In light of the

[7] See http://archive.eso.org/dss/dss.

similarity of the properties of the central stars of NGC 40 and BD +30 3639, the comparison between physical sizes and X-ray emission properties indicates that the former PN might best be considered as an evolved version of the latter. This interpretation places constraints on [WC] PN evolutionary schemes in which the central stars evolve from late to early [WC] spectral types (see Pena et al. [2001] and references therein). Specifically, given the subtle differences between the central star spectral types ([WC9] and [WC8], respectively) and wind properties of NGC 40 and BD +30 3639 (Leuenhagen et al. 1996), the contrast in their X-ray and optical/near-infrared properties indicates that [WCL] stars and their associated PNs may evolve between subclasses on timescales <5000 yr, i.e., a time period shorter than the approximate dynamical age of the hot bubble in NGC 40 (Akashi et al. 2006). We stress, however, that the notion that [WC] PN central stars evolve from late to early subtypes remains the subject of debate (Pena et al. 2001).

The upper limit on X-ray luminosity that we obtain for Hen 2-99 ($L_X < 5\times10^{30}$ ergs s^{-1}; § 2.2) constrains this nebula to be less X-ray luminous than all PNs thus far detected in X-rays (Soker & Kastner 2003; Kastner et al. 2003; Guerrero et al. 2005) with the exception of NGC 40 (this paper). The nondetection of Hen 2-99 by *Chandra* therefore would suggest either that the fast wind from the central ([WC9]) star has yet to collide with the ionized ejecta seen in optical images, or that any diffuse X-ray emission emanating from shocks produced by its fast wind has now faded to a level similar to or less than that detected in NGC 40. The former interpretation would appear to be more consistent with the lack of a clearly defined inner rim in Hen 2-99 in near-infrared images (Fig. 5), if the presence of such limb-brightened bubble structures in optical/near-infrared images of PNs is interpreted as evidence of wind-wind shocks. Additional X-ray observations of [WC] PNs with and without well-formed optical/near-infrared bubbles are required to test the hypothesis that the lack of detectable X-ray emission from Hen 2-99 indicates that this PN has yet to enter a phase of strong wind-wind shocks, despite the very large wind momentum of its central star.

This research was supported by NASA through Chandra award number GO4-5169X issued to Rochester Institute of Technology by the Chandra X-Ray Observatory Center, which is operated by Smithsonian Astrophysical Observatory for and on behalf of NASA under contract NAS8-03060. O. D. is grateful to Janet Jeppson Asimov for financial support.

Facilities: CXO (ACIS)

REFERENCES

Acker, A., Gorny, S. K., & Cuisinier, F. 1996, A&A, 305, 944
Akashi, M., Soker, N., & Behar, E. 2006, ApJ, submitted
Arnaud, K. 1996, in ASP Conf. Ser. 101, Astronomical Data Analysis Software and Systems V, ed. G. Jacoby & J. Barnes (San Francisco: ASP), 17
Arnaud, K., Borkowski, K. J., & Harrington, J. P. 1996, ApJ, 462, L75
Balick, B., & Hajian, A. R. 2004, AJ, 127, 2269
Chu, Y.-H., Guerrero, M. A., Gruendl, R. A., Williams, R. M., & Kaler, J. B. 2001, ApJ, 553, L69
Cox, P., Huggins, P. J., Maillard, J.-P., Habart, E., Morisset, C., Bachiller, R., & Forveille, T. 2002, A&A, 384, 603
Crowther, P. A., De Marco, O., & Barlow, M. J. 1998, MNRAS, 296, 367
De Marco, O., & Barlow, M. J. 2001, Ap&SS, 275, 53
Gorny, S. K., & Stasinska, G. 1995, A&A, 303, 893
Gorny, S. K., & Tylenda, R. 2000, A&A, 362, 1008
Guerrero, M. A., Chu, Y.-H., & Gruendl, R. A. 2002, A&A, 387, L1
Guerrero, M. A., Chu, Y.-H., Gruendl, R. A., & Meixner, M. 2005, A&A, 430, L69
Herwig, F. 2001, Ap&SS, 275, 15
Kaler, J. B., Shaw, R. A., Feibelman, W. A., & Lutz, J. H. 1989, ApJS, 70, 213
Kastner, J. H., Balick, B., Blackman, E. G., Frank, A., Soker, N., Vrtilek, S. D., & Li, J. 2003, ApJ, 591, L37
Kastner, J. H., Li, J., Vrtilek, S. D., Gatley, I., Merrill, K. M., & Soker, N. 2002, ApJ, 581, 1225
Kastner, J. H., Soker, N., Vrtilek, S. D., & Dgani, R. 2000, ApJ, 545, L57
Kastner, J. H., Vrtilek, S. D., & Soker, N. 2001, ApJ, 550, L189
Koesterke, L., Dreizler, S., & Rauch, T. 1998, A&A, 330, 1041
Kreysing, H. C., Diesch, C., Zweigle, J., Staubert, R., Grewing, M., & Hasinger, G. 1992, A&A, 264, 623
Leuenhagen, U., Hamann, & W.-R., Jeffery, C. S. 1996, A&A, 312, 167
Li, J., Harrington, J. P., & Borkowski, K. J. 2002, AJ, 123, 2676
Li, J., Kastner, J. H., Prigozhin, G. Y., & Schulz, N. S. 2003, ApJ, 590, 586
Martin, J., Xilouris, K., & Soker, N. 2002, A&A, 391, 689
Meaburn, J., Lopez, J. A., Bryce, M., & Mellema, G. 1996, A&A, 307, 579
Mendez, R. H., Kudritzki, R. P., Herrero, A., Husfeld, D., & Groth, H. G. 1988, A&A, 190, 113
Pena, M., Stasinska, G., & Medina, S. 2001, A&A, 367, 983
Perinotto, M., Cerruti-Sola, M., & Lamers, H. J. G. L. M. 1989, ApJ, 337, 382
Pottasch, S., Wesselius, P. R., Wu, C.-C., & van Duinen, R. J. 1977, A&A, 54, 435
Sahai, R., Kastner, J. H., Frank, A., Morris, M., & Blackman, E. G. 2003, ApJ, 599, L87
Soker, N. & Kastner, J. H. 2003, ApJ, 583, 368
Swings, P. 1940, ApJ, 92, 289